COMPOSITE-BASED APPROACH FOR STRAIN-RATE SENSITIVITY OF STRESS-STRAIN CURVES OF CEMENT-MATRIX COMPOSITES

Huang Hsing Pan[1] - Professor; **Jung-Cheng Lin**[1] – Graduate Student; **Yu Wen Liu**[2] - Professor

[1]Dept. of Civil Engineering, National Kaohsiung University of Applied Sciences, Kaohsiung, Taiwan - 807

[2]Dept. of Civil and Water Resources Eng., National Chiayi University, Chiayi, Taiwan - 300

***ABSTRACT**: Based on a four-parameter model and the inclusion theory with the secant moduli method, a composite-based approach is developed to investigate the stress-strain behavior of the mortar with different strain rates from 5×10^{-6}/s to 10^{-1}/s. According to Burgers' rheological model, four material parameters are determined to simulate the stress-strain curves of the binder first. These parameters are sensitive to applies strain rates and originally simulated from the experimental curves of the binder. Then, the mean-field approach combining with a secant-moduli method is established to predict stress-strain curves of mortar and verified by experiments. Results show that the stress-strain curves of the simulation and the experiments are pretty close to the each other with different strain rates, no matter what the linear or the nonlinear part of the curves up to 90% peak strength.*

***KEYWORDS**: Stress-strain curve, rate-dependent, overall properties, Burgers' model*

1. INTRODUCTION

The strain-rate sensitive behavior of cement-based materials has been investigated for many years [1-5]. With increasing strain rates, the peak strength, the initial elastic Young modulus and the initial Poisson's ratio increase under tension and compression, as opposed to the strain at the peak stress first decreases and then increases [1]. Less microcracking would be one of the reasons for the higher peak strength with an increase of strain rates [2], and also for the initial elastic Young modulus and the initial Poisson's ratio at the strain levels calculated. Meanwhile, the dynamic behavior of cement-based materials due to applied strain rates depends on the existing defects, moisture condition, water-to-binder ratio, the volume fraction of the aggregate and the loading conditions, but the physical cause of strain-rate sensitivity is not completely understood.

Some numerical and theoretical models were presented to describe the effect of strain rates in concrete materials or composites, for instance, Brara *et al* [4] proposed an experimental technique based on the Hopkinson bar principle combined with the spalling phenomenon and numerical simulations by means of discrete element method to analyze on concrete at high strain rate in tension. Chandra and Krauthammer [6] using a structural dynamics point of view to examine the strain-rate effect in cement-matrix composite. The ADINA concrete model based on a uniaxial stress-strain relationship was also chosen to account for high strain-rate effects from 10^{-7} /sec to 10^{3}/sec [7-9]. A characterized technique with the peak load method was proposed to quantify dynamic fracture properties of quasi-brittle materials [10-11]. Ragueneau and Gatuingt [12] developed the concrete constitutive model to account for substantial difference of inelastic

response in tension and compression. Among them, the strain-rate effect of the cement-based materials simulated by theoretical models or numerical calculations seldom considered the properties of the individual phases but those of the composite materials.

The composite-based approach here is developed and concentrates on the stress-strain curves of the cement-matrix material with seven strain rates from 5×10^{-6}/s to 10^{-1}/s so that the simulated results can be calculated from the constitutions without having to determine the material properties of the composite for each and every case. Three mortars at the material age of 28 days are made to compare with and verify the stress-strain curves of predicted results.

2. MATERIALS AND EXPERIMENTS

To simulate the stress-strain curves of the mortar with different strain rates, the stress-strain relation of the aggregate is assumed to be linear, but the mortar and the binder have nonlinear stress-strain relations. All of them are strain rate-dependent, and seven strain rates with 5×10^{-6}/s, 1×10^{-5}/s, 7.22×10^{-5}/s, 1×10^{-4}/s, 1×10^{-3}/s, 1×10^{-2}/s and 1×10^{-1}/s are chosen to test the materials here, where the strain rate 7.22×10^{-5}/s is converted from ASTM C39 with $\phi15\times30$cm specimen at the loading velocity 1.3mm/min.

The bind is Type I Portland cement with a 0.45 water-to-cement ratio (w/c), and the aggregate is the sand consisting of 99% quartz. The measured particle size of the quartz sand was 0.7~1.0mm, a specific gravity of 2.65, absorption 0.24%, and a shape similar to a spheroid with an aspect ratio $\alpha=1.13$ approximately. The elastic bulk and shear moduli of the sand at the strain rate $\dot{\varepsilon}=1\times10^{-5}$/s are $\kappa_1=19.46$GPa and $\mu_1=18.44$GPa, respectively. The experimental Young modulus, E_1, of the sand containing different strain rates is shown in Table 1, and all Poisson ratios are assumed to have a constant value with $\nu_1=0.14$ at $\dot{\varepsilon}=1\times10^{-5}$/s for convenience. Mortars with three volume fractions of sand are $c_1=0.3$, 0.4 and 0.5 respectively, and mixture proportions are shown in Table 2, where the material at $c_1=0$ represents the cement paste.

Table 1- Young elastic modulus of the sand

Strain rate	5×10^{-6}/s	1×10^{-5}/s	7.22×10^{-5}/s	1×10^{-4}/s	1×10^{-3}/s	1×10^{-2}/s	1×10^{-1}/s
E_1(GPa)	40.3	42.0	44.5	47.5	50.0	53.3	58.4

Table 2- Mixture proportions of mortar (kg/m^3)

c_1	w/c	cement	water	sand
0	0.45	1302	586	—
0.3	0.45	912	410	795
0.4	0.45	782	352	1060
0.5	0.45	652	293	1325

Cylindrical test specimens were prepared using steel molds. Twelve samples were made at each strain rate. At the slowest strain rate, specimens failed in approximate 60 min, and at the fastest strain rate failed in 0.2 sec. The specimens were tested at the material age of 28 days, and the sample was dried in the air one day before the test. The longitudinal and lateral strains were measured to plot the stress-strain curves of the binder and the mortar to calculate the initial Poisson ratio and examine the simulated results of the developed approach.

3. BURGERS' FOUR-PAPAMETER MODEL FOR STRAIN-RATE SENSITIVITY

Burgers' four-parameter rheological model with two springs and two dashpots has been use to determine the stress-strain behavior of the cement binder by considering the effect of the strain rate $\dot{\varepsilon}$ as shown in Fig. 1, where two springs and two dashpots are four parameters denoted as $k_1(\dot{\varepsilon})$, $k_2(\dot{\varepsilon})$, $\eta_1(\dot{\varepsilon})$ and $\eta_2(\dot{\varepsilon})$ respectively. The binder subjected to an external load $f(t)$, where t is the loading time, will take place the displacements δ_1, δ_2, and δ_3 at k_1, η_1, and k_2 and η_2, respectively. Noting that the total loading velocity $w = \dot{\delta}_1 + \dot{\delta}_2 + \dot{\delta}_3$.

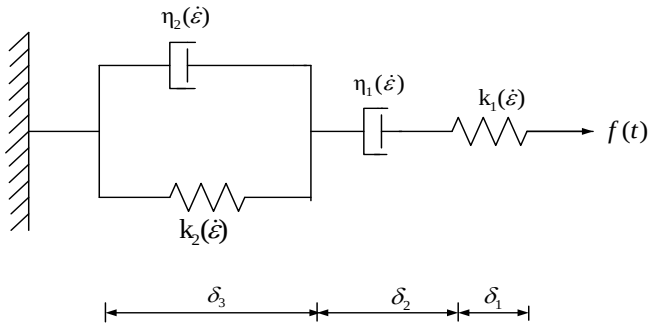

Fig. 1- Burgers' model for the binder depending on strain rate

The constitutive equation of the cement binder with w/c=0.485 under $\dot{\varepsilon} = 1\times10^{-5}$/s has been derived and determined [13]

$$\frac{\sigma}{f_p} = 3.71\left[e^{m_1(\varepsilon\times10^3)} - 1.009e^{m_2(\varepsilon\times10^3)}\right] + 0.0334 \tag{1}$$

where σ and f_p are the stress and the peak stress of the cement binder, respectively, whereas m_1 and m_2 are the characteristic roots depending on four parameters.

4. MICROMECHANICS-BASED MODEL FOR STRAIN-RATE SENSITIVITY

The mechanics-based approach we developed proceeds to calculate the elastic behavior of the two-phase composite first. Here the Eshelby-Mori-Tanaka [14-15] theory is recaptured to determine the effective elastic properties of the two-phase composite containing three-dimensional randomly oriented, ellipsoidal inclusions. This method calls for the introduction of a homogeneous comparison material. The explicit forms of the effective elastic bulk and shear moduli for the isotropic composites with ellipsoidal inclusions are recaptured as

$$\kappa = \frac{\kappa_0}{1 + c_1(p_2 / p_1)}; \quad \mu = \frac{\mu_0}{1 + c_1(q_2 / q_1)} \tag{2}$$

where κ and μ are the effective elastic bulk and shear moduli of the composite, respective, and the material constants, p_1, p_2, q_1 and q_2, follow the same material parameters as previously [16]. However, the stress-strain curve of the cement-matrix composite calculated from the

effective elastic moduli in (2) is always linear and independent of strain rate, which can not reflect a nonlinear stress-strain behavior of the cementitious materials.

To rebuild the stress-strain behavior from the linear relation to nonlinear one, we use the secant moduli instead of the elastic moduli to simulate the binder and the cement-matrix composite. As secant moduli of the binder continue to decrease in the course of deformation at a given strain rate $\dot{\varepsilon}$, their values are smaller than their elastic counterparts, such as

$$\kappa_0^s(\varepsilon,\dot{\varepsilon}) \le \kappa_0(\varepsilon,\dot{\varepsilon});\ \mu_0^s(\varepsilon,\dot{\varepsilon}) \le \mu_0(\varepsilon,\dot{\varepsilon}) \tag{3}$$

where the superscript "s" stands for the secant moduli, which are the direct ratio of the stress to the total strain in definition.

When the isotropic composite is subjected to a uniaxial stress $\bar{\sigma}_{11}$ only, so as to induce the applied strain ε_{11}^0. When the stress-strain curve of the binder (comparison material) is simulated by the Burgers' four-parameter model at given strain rate $\dot{\varepsilon}$, the secant Young modulus of the binder, E_0^s, is determined from its basic definition at a given stage of strain or stress

$$E_0^s(\varepsilon,\dot{\varepsilon}) = \bar{\sigma}_{11}(\varepsilon,\dot{\varepsilon})/\varepsilon \tag{4}$$

where $\varepsilon = \varepsilon_{11}^0$ the axial strain in the 1-axis.

Then, the explicit forms of the effective secant moduli of the cement-matrix composite are modified from (2) by replacing κ_0 and μ_0 by $\kappa_0^s(\varepsilon,\dot{\varepsilon})$ and $\mu_0^s(\varepsilon,\dot{\varepsilon})$, respectively, and the forms become.

$$\kappa^s(\varepsilon,\dot{\varepsilon}) = \frac{\kappa_0^s(\varepsilon,\dot{\varepsilon})}{1+c_1(p_2/p_1)};\ \ \mu^s(\varepsilon,\dot{\varepsilon}) = \frac{\mu_0^s(\varepsilon,\dot{\varepsilon})}{1+c_1(q_2/q_1)} \tag{5}$$

To simulate the stress-strain curve of the cement-based composite, one can directly plot the overall stress-strain curve subjected to a uniaxial strain ε (is equal to ε_{11}^0 here) through

$$\bar{\sigma}_{11}(\varepsilon,\dot{\varepsilon}) = E^s(\varepsilon,\dot{\varepsilon})\cdot\bar{\varepsilon}_{11}(\varepsilon,\dot{\varepsilon}) \tag{6}$$

at a given strain rate $\dot{\varepsilon}$, and by assuming the strain ε from 0 to the peak strain of the binder, where E^s and $\bar{\varepsilon}_{11}$ are the overall effective secant Young modulus and effective strains of the composite respectively. Then, the predicted overall stress-strain curve of the composite is plotted along the point $(\bar{\varepsilon}_{11},\bar{\sigma}_{11})$ in the coordinate.

5. RESULTS AND DISCUSSION

The peak stress and its corresponding strain of the paste and mortar are also shown in Table 3. The initial Poisson ratio of the binder ν_0 and the mortar ν are tested and shown in Table 4. Those values do not change much with increasing strain rates because the testing conditions of the specimen and the calculation of initial Poisson's ratio are different from previous report [1].

Table 3- Peak stress and its corresponding strain of cement-based materials

Strain rate	$c_1 = 0$		$c_1 = 0.3$		$c_1 = 0.4$		$c_1 = 0.5$	
	Peak stress (MPa)	Peak strain (10^{-3})	Peak stress (MPa)	Peak strain (10^{-3})	Peak stress (MPa)	Peak strain (10^{-3})	Peak stress (MPa)	Peak strain (10^{-3})
5×10^{-6}/s	46.95	6.06	50.11.	4.68	52.40	4.22	52.53	3.91
1×10^{-5}/s	47.91	5.51	52.32	4.59	54.22	4.15	54.22	3.70
7.22×10^{-5}/s	54.89	4.60	56.19	3.45	58.71	3.22	58.18	2.93
1×10^{-4}/s	56.15	4.38	57.06	3.45	61.48	3.20	57.78	2.51
1×10^{-3}/s	58.61	3.77	65.59	3.21	65.57	3.14	61.22	2.37
1×10^{-2}/s	64.30	3.46	75.74	3.00	76.18	2.72	65.40	2.18
1×10^{-1}/s	69.03	2.28	77.99	2.95	78.56	2.66	71.89	2.10

Table 4- Initial Poisson's ratio of cement-based materials

Strain rate	$c_1 = 0$	$c_1 = 0.3$	$c_1 = 0.4$	$c_1 = 0.5$
5×10^{-6}/s	0.183	0.174	0.171	0.169
1×10^{-5}/s	0.183	0.174	0.171	0.169
7.22×10^{-5}/s	0.182	0.173	0.171	0.167
1×10^{-4}/s	0.182	0.172	0.168	0.166
1×10^{-3}/s	0.182	0.172	0.168	0.166
1×10^{-2}/s	0.181	0.171	0.167	0.165
1×10^{-1}/s	0.180	0.170	0.166	0.164

The experimental stress-strain curves of the binder with solid lines are shown in Fig. 2, and were simulated by Burgers' four-parameter model with the dotted lines, where the four material parameters in terms of the strain rate with sample correlation coefficients $r = 0.99$ are

$$k_1(\dot{\varepsilon}) = 0.23\cdot(\log\dot{\varepsilon})^2 + 0.39\cdot\log\dot{\varepsilon} + 0.19 \tag{7}$$

$$k_2(\dot{\varepsilon}) = -0.04\cdot(\log\dot{\varepsilon})^2 - 1.20\cdot\log\dot{\varepsilon} + 4.75 \tag{8}$$

$$\eta_1(\dot{\varepsilon}) = 0.21\cdot(\log\dot{\varepsilon})^2 + 0.56\cdot\log\dot{\varepsilon} + 0.36 \tag{9}$$

$$\eta_2(\dot{\varepsilon}) = -3.98\cdot(\log\dot{\varepsilon})^2 - 14.05\cdot\log\dot{\varepsilon} + 175.16 \tag{10}$$

Four parameters in (7)-(10) are suitable for the binder with w/c=0.45 and the strain rates between 5×10^{-6}/s and 1×10^{-1}/s. Those simulated results of the stress-strain curve of the binders allow us to easily obtain the secant Young modulus of the binder during the deformation.

From (6), the stress-strain curves of the mortars containing $c_1 = 0.3$, 0.4 and 0.5, are simulated, and the results are depicted in Figs. 3-5. Figs. 3-5 show that the stress-strain curves of the simulation and the experiments are pretty close to the each other with different strain rates, no matter what the linear or the nonlinear part of the curves. Thus, the proposed approach by combining the Burgers' model with the inclusion theory and the secant moduli method is seemly suitable for the stress-strain relations of the cement-based composites in low and middle strain rate dynamics.

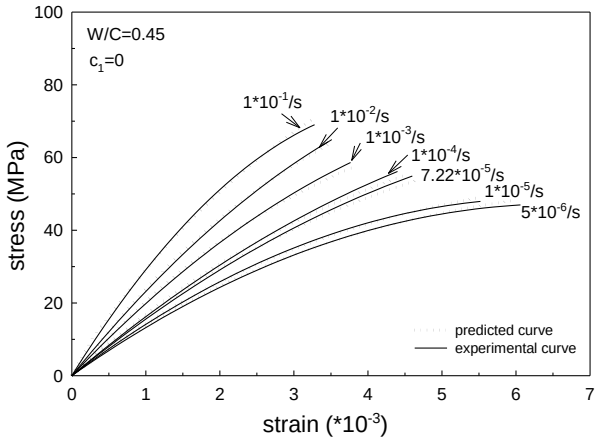

Fig. 2- Experiments and Burgers' model for binder with w/c=0.45.

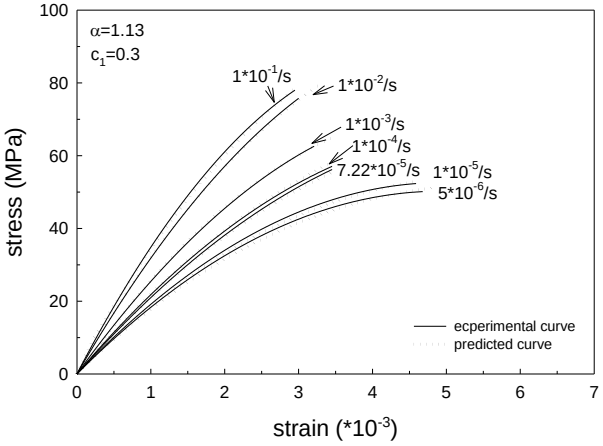

Fig. 3- Experiments and simulations for $c_1 = 0.3$ mortar.

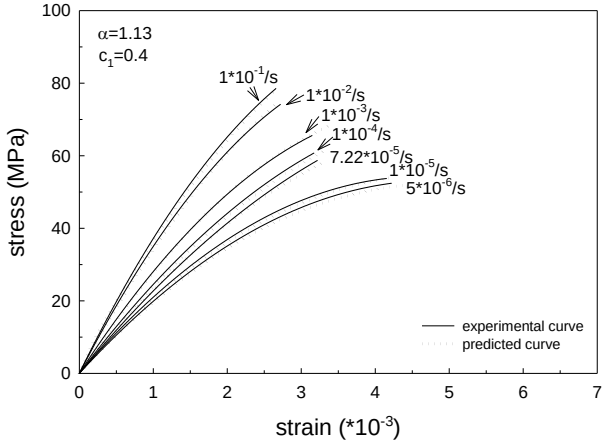

Fig. 4- Experiments and simulations for $c_1 = 0.4$ mortar.

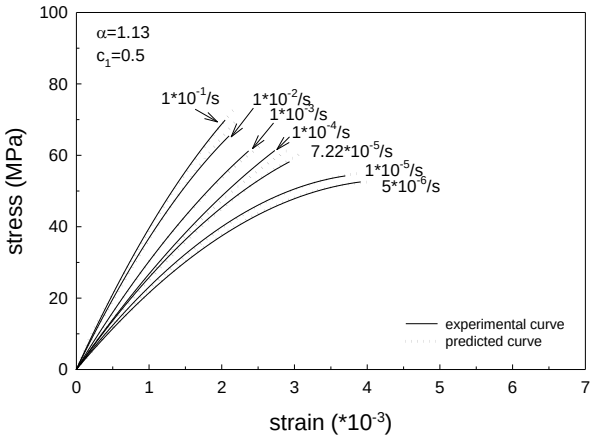

Fig. 5- Experiments and simulations for $c_1 = 0.5$ mortar.

6. CONCLUDING REMARDS

Four parameters based on Burgers' model in terms of the strain rate are found to reproduce the stress-strain curves of the binder when the strain rate lies in the range between 5×10^{-6}/s to

1×10^{-1}/s. From the experimental and numerical results, the developed composite-based approach based on the Burgers' four-parameter model and the inclusion theory with secant moduli method are proved to be able to account for the rate-sensitivity of stress-strain curves in mortar, and the predicted stress-strain curves calculating from the proposed approach are in an acceptable range of accuracy until the park stress reaches. The simulated results are good for the overall stress-strain curves of the cement-based materials.

REFERENCES

1. Harsh, S, Shen, Z., and Darwin, D. (1990), *Strain-rate sensitive behavior of cement paste and mortar in compression*, ACI Materials J., Vol. 87, 508-515.
2. Yon, J-H, Hawkins, N. M., and Kobayashi, A. S. (1992), *Strain-rate sensitivity of concrete mechanical properties*, ACI Material J., Vol. 89, 146-153.
3. Hsiao, H. M., and Daniel, I. M. (1998), *Strain rate behavior of composite materials*, Composites, Part B, 29B, 521-533.
4. Brara, A., Camborde, F., Klepaczko, J. R., and Mariotti, C. (2001), *Experimental and numerical study of concrete at high strain rate in tension*, Mechanics of Materials, Vol. 33, 33-45.
5. Cao, J., and Chung, D. D. L. (2002), *Effect of strain rate on cement moratr under compression, studied by electrical resistivity measurement*, Cement and Concrete Research, Vol. 32, 817-819.
6. Chandra, D., and Krauthammer, T. (1995), *Strength enhancement in particulate solids under high loading rate*, Earthquake Engineering and Structural Dunamics, Vol. 24, 1609-1622.
7. Bath, K. J., and Ramaswamy, S. (1979), *On three-dimensional nonlinear analysis of concrete structures, nuclear engineering and design*, Vol. 52, 385-409.
8. ADINA R&D Inc. (1987), *A finite element computer program for automatic dynamic incremental nonlinear analysis*, Report ARD 87-1, ADINA R&D, Watertown, MA.
9. Tedesco, J. W., Powell, J. C., Ross, C. A., and Hughes, M. L. (1997), *A strain-rate-dependent concrete material model for ADINA*, Computers and Structures, Vol. 64, 1053-1067.
10. Tang, T., Ouyang, C., and Shah, S. P. (1996), *A simple method for determining material fracture parameters from peak loads*, ACI Materials J., Vol. 93, 147-157.
11. Lambert, D. E., and Ross, C. A. (2000), *Strain rate effects on dynamic fracture and strength*, Int. J. Impact Engineering, Vol. 24, 985-998.
12. Ragueneau, F., and Gatuingt, F. (2003), *Inelastic behavior modelling of concrete in low and high strain rate dynamics*, Computers and Structures, Vol. 81, 1287-1299.
13. Kuo, T.-H., Pan, H. H., and Weng, G. J. (2008), *Micromechanics-based predictions on the overall stress-strain relations of cement-matrix composites*, ASCE, J. Engineering Mechanics. (in press)
14. Eshelby, J. D. (1957), *The determination of the elastic field of an ellipsoidal inclusion, and related problems*, Proc. Roy. Soc., London A241, 376-396.
15. Mori, T. and Tanaka, K. (1973), *Average Stress in Matrix and Average Elastic Energy of Materials with Misfitting Inclusions*, Acta Metall., Vol. 21, 571-574.
16. Pan, H. H., and Weng, G. J. (1995), *Elastic moduli of heterogeneous solids with ellipsoidal inclusions and elliptic cracks*, Acta Mechanica, Vol. 110, 73-94.